

## Shear-Induced Orientational Transitions in the Body-Centered Cubic Phase of a Diblock Copolymer Gel

I. W. Hamley\* and J. A. Pople

*School of Chemistry, University of Leeds, Leeds LS2 9JT, U.K.*

J. P. A. Fairclough and A. J. Ryan

*Department of Chemistry, University of Sheffield, Sheffield S3 7HF, U.K.*

C. Booth and Y.-W. Yang

*Department of Chemistry, University of Manchester, Manchester M13 9PL, U.K.*

*Received October 23, 1997; Revised Manuscript Received February 3, 1998*

**ABSTRACT:** Gels of a poly(oxyethylene)–poly(oxybutylene) diblock copolymer in aqueous solution forming a bcc phase have been examined using small-angle X-ray scattering (SAXS) with simultaneous rheology. Application of large amplitude oscillatory shear is observed to induce macroscopic alignment of twinned bcc crystals. Alignment at relatively low frequency leads to a structure in which {200} planes are oriented normal to the shear direction. At high frequency, large amplitude shearing leads to a transition to flow with the [111] plane parallel to the shear direction. Flow occurs in the {110} and {211} planes which intersect along the same [111] direction, leading to a high-symmetry SAXS pattern with numerous sharp reflections. These results highlight the similarity between the defect mechanics of cubic phases in block copolymer gels and those in metals.

### Introduction

Self-organization of block copolymers in the melt leads to the formation of lamellar, hexagonal-packed cylindrical, cubic-packed spherical, and bicontinuous cubic structures.<sup>1,2</sup> Structures with these symmetries have also been observed in concentrated solutions of block copolymers.<sup>1</sup> In this case, the structures are lyotropic liquid crystal phases where polymer concentration is also a relevant variable in the phase behavior. In more dilute solutions, block copolymer micelles exist in an unassociated phase termed a micellar solution. The formation of ordered structures such as cubic micellar phases can be described in terms of the volume fraction of spheres. For example, assuming that the micelles are hard spheres, a bcc phase is expected to have a volume fraction of spheres,  $\Phi = 0.68$ . The phase behavior of block copolymers in solution is expected to differ from that of block copolymer melts due to the presence of interactions between the monomers and solvent in addition to unfavorable monomer–monomer interactions. In concentrated solutions where micellar coronas overlap, the corona blocks are osmotically required to maintain a uniform concentration in the matrix phase (containing solvent and corona segments). This requirement places entropic restrictions on the coronal block conformation and micelles pack in cubic structures to minimize the osmotic constraint.<sup>3</sup> In contrast, the formation of cubic phases of spherical domains in block copolymer melts is controlled by the balance of interfacial free energy and the free energy associated with packing constraints (which tend to favor uniform thickness domains) with an additional entropic penalty resulting from chain stretching. Cubic phases with spherical microdomains in block copolymer melts can thus be accessed by selecting a highly asymmetric copolymer.<sup>2,4</sup>

The development of cubic ordering in a micellar solution is accompanied by a profound change in the flow behavior. Whereas micellar solutions flow under their own weight and are viscoelastic (or even Newtonian) fluids, cubic phases are elastic solids, with a finite yield stress. Cubic phases in block copolymer solutions have thus been characterized as “hard gels”.<sup>5</sup> Gel formation in aqueous solutions of poly(oxyethylene)–poly(oxypropylene)–poly(oxyethylene) (EPE) (commercial name: Pluronic) copolymers in aqueous solution has also been correlated with the association of micelles into a cubic phase.<sup>6</sup> Mortensen and co-workers<sup>7–9</sup> have used shear to prepare aligned domains of Pluronic block copolymer gels, the structure of which was elucidated using small-angle neutron scattering (SANS). Of particular interest is the observation of a “cubatic” phase in a gel formed by Pluronic F88 (E<sub>97</sub>P<sub>39</sub>E<sub>97</sub>, where the subscripts denote the number of repeat units).<sup>8</sup> A SANS pattern from a “single-crystal” bcc array (obtained by steady shear) was obtained in which the positional correlation length was not more than 5–10 lattice constants. This structure was thus described as being characterized by only quasi-long-range positional order, but long-range correlations in the orientation of unit cell edges. The phase behavior of Pluronic triblocks, including concentrated solutions where liquid crystalline phases have been observed, has recently been reviewed.<sup>1,10,11</sup>

The gelation of poly(oxyethylene)–poly(oxybutylene) (EB) diblocks has been investigated using tube inversion, polarized light microscopy, rheometry, and DSC.<sup>12</sup> It has been noted that whereas EB diblocks formed a gel under appropriate conditions of polymer concentration and temperature, EBE and BEB triblocks did not.<sup>13</sup> However, a triblock with a higher PEO content was found to gel.<sup>14,15</sup> Gelation in PEO–poly(DL-lactide) diblocks<sup>16</sup> and PEO–poly(methylene) diblocks has also been examined.<sup>17</sup> The phase behavior of solutions of a

\* Author for correspondence.

commercial EB diblock (a product of Dow Chemical) in solution in water/oil mixtures has recently been examined, using SAXS and deuterium NMR measurements.<sup>18</sup> A remarkably rich structural polymorphism was noted for the ternary system.

The influence of shear on the bcc phase in block copolymer melts has been probed using SANS on samples oriented using reciprocating shear.<sup>19,20</sup> Almdal and co-workers showed that highly twinned bcc single crystals could be obtained by large amplitude shearing.<sup>19</sup> The deformation occurred via slip of close-packed {110} slip planes in the  $[\bar{1}11]$  direction. The shear gradient direction was coincident with  $[0\bar{1}1]$ . Epitaxial growth of a bcc structure from an oriented hexagonal structure has been observed for two polyolefin diblocks.<sup>17</sup> A  $\langle 111 \rangle$  direction of the bcc structure was found to be coincident with the original cylinder axis, leading to a highly oriented, twinned bcc structure. At high and low shear rates, twinned bcc crystals were observed. However, at intermediate shear rates, shear melting occurred as shown by isotropic two-dimensional SAXS patterns. The loss of translational order at intermediate shear rates was ascribed to the generation of numerous defects, i.e., a proliferation of slip or {110} planes.

We have previously investigated the phase behavior of gels of a poly(oxyethylene)–poly(oxybutylene) (EB) diblock,  $E_{40}B_{10}$  in 0.2 M  $K_2SO_4$ , elucidated using SAXS with simultaneous rheology.<sup>21</sup> This complemented earlier work where micellar dimensions and association numbers were characterized using light scattering, gel–sol boundaries were elucidated via mobility experiments and clouding was observed at high temperatures.<sup>22</sup> Both fcc and bcc phases were identified using SAXS, with the bcc phase observed for concentrations of 30 wt % polymer and above at low temperatures. However, the effect of shear on the bcc phase was not investigated in our earlier papers.

Here, the effect of shear on the orientation of the bcc phase formed in solutions of the diblock  $E_{86}B_{10}$  in 0.2 M  $K_2SO_4$  is examined. The sample was sheared in a commercial rheometer, modified for simultaneous SAXS and rheology experiments on samples subject to oscillatory shear. The orientation identified differs from that previously reported for block copolymer melts,<sup>19</sup> Pluronic triblocks in aqueous solution,<sup>7,8</sup> and poly(styrene)–poly(isoprene) diblocks in a selective solvent.<sup>23</sup> Furthermore, a rich phenomenology of transitions as a function of shear rate and amplitude is elucidated.

## Experimental Section

**1. Materials.** The copolymer was prepared by sequential anionic polymerization of ethylene oxide followed by 1,2-butylene oxide. The initiator was diethylene glycol monomethyl ether partly in the form of its potassium salt: mole ratio  $[OH]/[K] \approx 10$ . Characterization of the first-formed poly(oxyethylene) with gel permeation chromatography (GPC, calibrated with poly(oxyethylene) standards) gave  $M_{pk} \approx 3800$  g mol<sup>-1</sup> and  $M_w/M_n = 1.02$ , while comparison of the intensities of resonances from backbone and end group carbons in the <sup>13</sup>C NMR spectrum gave  $M_n = 3780$  g mol<sup>-1</sup>, consistent with chain length  $E_{86}$ . Similarly, characterization of the final copolymer gave  $M_w/M_n = 1.04$  (GPC),  $M_n = 4500$  g mol<sup>-1</sup> (NMR), and 90 mol % E (NMR), consistent with molecular formula  $E_{86}B_{10}$ . The intensities of resonances from end and EB-junction carbons were identical within experimental error, thus confirming the diblock structure. To ensure purity, the copolymer was extracted with hexane, and the composition was unchanged. Full descriptions of these procedures can be found in previous publications.<sup>13,24</sup>

The materials studied were concentrated solutions of the copolymer in 0.2 mol dm<sup>-3</sup>  $K_2SO_4$ , which were prepared by mixing at  $T = 60$ – $70$  °C, followed by several days of storage of the gel in a refrigerator. Aqueous  $K_2SO_4$  was used as a solvent in previous studies of gels of copolymer  $E_{40}B_{10}$ , since the gel phases of interest formed at conveniently accessible temperatures in that system.<sup>21,22</sup> For purposes of comparability, the same solvent was used in this work.

All experiments reported in this paper were conducted on a 40 wt % gel at 20 °C. The effect of shear on gels with 25, 27.5, 30, and 37.5 wt % copolymer was also examined. In general, the results were qualitatively similar to those presented here for the highest concentration gel examined. The extent of orientation induced by shear was found to increase as a function of copolymer concentration, as noted earlier for the  $E_{40}B_{10}$  system.<sup>21</sup> Furthermore, the X-ray scattering contrast increases with copolymer concentration, producing better SAXS patterns as presented herein.

**2. Simultaneous Small-Angle X-ray Scattering and Rheology.** At the Synchrotron Radiation Source, Daresbury Laboratory, U.K., SAXS experiments were conducted on beamline 8.2. This beamline is configured with an X-ray wavelength  $\lambda = 1.5$  Å. Details of the storage ring, radiation, camera geometry, and data collection electronics have been given elsewhere.<sup>25</sup> Scattered photons were collected on a multiwire gas-filled area detector. A scattering pattern from an oriented specimen of wet collagen (rat-tail tendon) was used for calibration of the  $q$  scale range of the detector, ( $q = 4\pi(\sin\theta)/\lambda$ , where the scattering angle is defined as  $2\theta$ ). The experimental data were corrected for background scattering (from the camera and empty shear cell), sample absorption, and the positional alinearity of the detector. Rheological measurements were performed using a Rheometrics Solids Analyzer RSA II system with a shear sandwich geometry. The rheometer generates an oscillatory (sinusoidal) deformation and the dynamic and loss shear moduli, respectively  $G'$  and  $G''$ , are measured as a function of the deformation conditions. Apertures were machined into the plates of the shear sandwich assembly to allow transmission of the X-ray beam and were covered by Kapton windows of 6 mm thickness, as described previously.<sup>18</sup> The shear sandwich was contained in an insulated oven, with temperature control to  $\pm 1$  °C. With the rheometer in situ at the X-ray beamline the shear direction  $\mathbf{v}$  was vertical, and the X-ray beam was incident along the horizontal shear gradient direction  $\nabla$ , the neutral direction  $\mathbf{e} = \nabla \times \mathbf{v}$  also being horizontal. The acquisition of SAXS and rheology was synchronized using an electronic trigger. The SAXS data counting time, 30 s per frame, was equal to the acquisition time for the dynamic mechanical measurements. Measurements at this time resolution can only be achieved at relatively high frequencies, due to the requirement imposed by the rheometer software that a sufficient number of strain cycles are completed. Furthermore, such measurements require a synchrotron source of X-rays.

## Results and Discussion

**1. Rheology.** The linear viscoelastic regime for the gel was determined by performing a “strain sweep” at a fixed frequency, as illustrated in Figure 1. This indicates linear behavior up to approximately 1% strain. Except in the case where large amplitude shearing was employed to align the specimen, rheological experiments were performed in the linear viscoelastic regime (at  $\lambda = 0.3\%$ ). A frequency sweep (taken after large amplitude oscillatory shear, with the sample in the ultimate alignment described below) is shown in Figure 2. This shows that  $G''$  is independent of frequency over the 4 orders of magnitude examined and that  $G'$  is larger than  $G''$  and a weakly increasing function of  $\omega$ . These results are consistent with a solidlike response over the range of frequencies accessible in the rheometer. It is possible that  $G'$  and  $G''$  are tending toward a crossover at lower

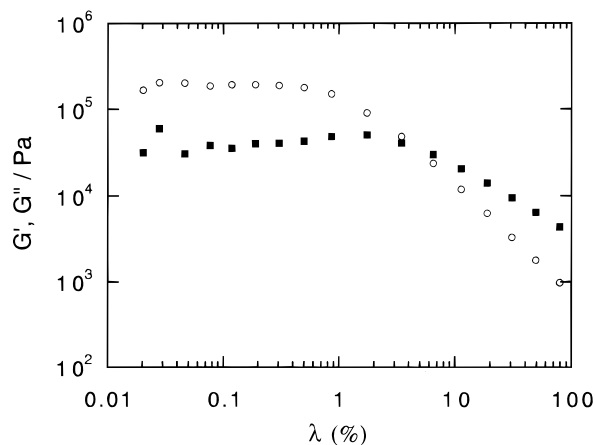


**Figure 1.** Dependence of the dynamic elastic moduli on strain amplitude at a fixed frequency ( $\omega = 1 \text{ rad s}^{-1}$ ): (○)  $G'$ , (■)  $G''$ .

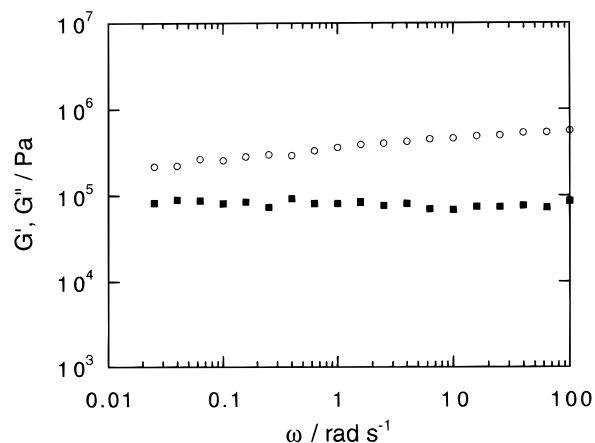


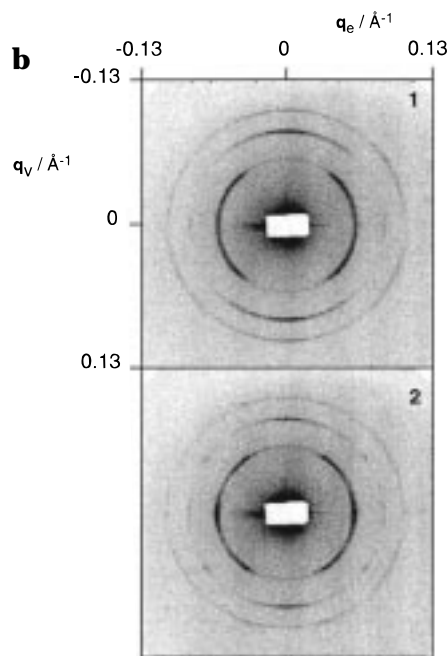
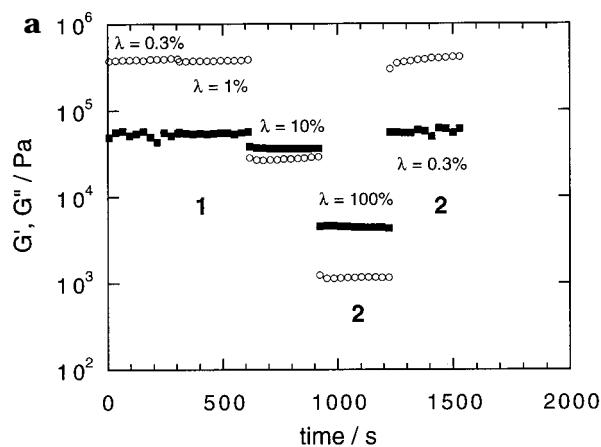
**Figure 2.** Dependence of the dynamic shear moduli [(○)  $G'$ ; (■)  $G''$ ] on frequency, with  $\lambda = 0.3\%$ .

frequencies, but this cannot be confirmed within the available frequency range.

**2. SAXS on Sheared Gel.** SAXS patterns for oriented gels are illustrated in Figures 3 and 4. The SAXS pattern for the as-mounted specimen contained unoriented rings in the positional ratio  $1:\sqrt{2}:\sqrt{3}$  (the absence of initial orientation is shown in Figure 5). This is consistent with the bcc (spacegroup  $Im\bar{3}m$ ) structure commonly observed for melts of highly asymmetric block copolymers and in surfactant micellar solutions.

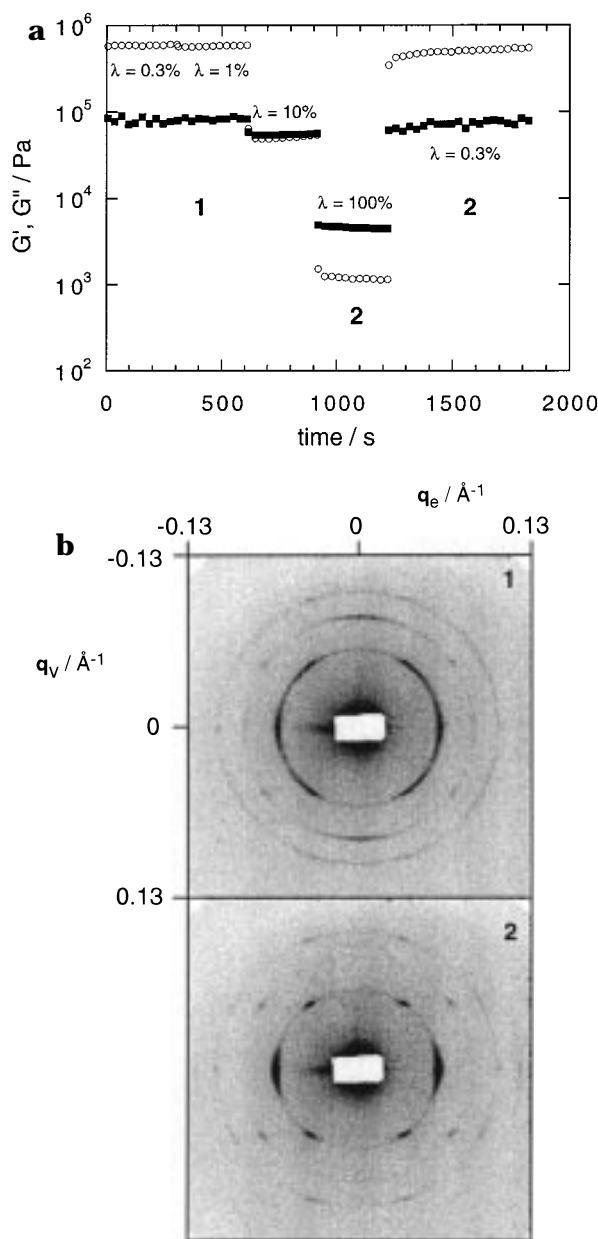
The effect of increasing the amplitude of oscillatory shear on the alignment of the bcc phase was investigated as follows. Strain was applied at a fixed frequency in a series of steps, each lasting 5 min. The strain was successively increased from  $\lambda = 0.3\%$  (linear response) to 1% to 10% to 100%, and then the sample was allowed to relax back to a quiescent state (with measurements of the dynamic moduli at  $\lambda = 0.3\%$ ). The results are plotted as  $G'$ ,  $G''$  as a function of time in Figures 3a and 4a with SAXS patterns corresponding to particular regimes in Figures 3b and 4b.

Figure 3 contains results for strain steps at  $\omega = 10 \text{ rad s}^{-1}$ . The onset of nonlinear viscoelastic response is apparent above 1% strain.<sup>26</sup> At  $\lambda = 10\%$ , the apparent  $G''$  was larger than  $G'$ , and both  $G'$  and  $G''$  decreased as the strain was increased, showing that the gel was shear thinning. The symmetry of the SAXS patterns, however, was unaltered up to frame 30–32, over which range a transition was observed to a structure with the SAXS pattern shown in part 2 of Figure 3b. The



**Figure 3.** (a) dynamic shear moduli [(○)  $G'$ ; (■)  $G''$ ] from simultaneous SAXS/rheology experiments for the gel subjected to different strain amplitudes (indicated) at a frequency  $\omega = 10 \text{ rad s}^{-1}$ . (b) SAXS patterns obtained concurrently, corresponding to the rheology as indicated by regime 1 or 2.

interpretation of these SAXS patterns is discussed below. Since the SAXS acquisition time was 30 s, the midpoint of the transition occurred at 930 s, which corresponds precisely to the onset of shearing at  $\lambda = 100\%$ . This correlation indicates that the transition induced by shear at the largest amplitude examined occurs rapidly (within approximately 30 s). Remarkably, cessation of large amplitude shear led to the rapid (within 30–60 s) recovery of the original values of  $G'$  and  $G''$  (measured in the linear viscoelastic regime). However, this was not accompanied by a transition in the SAXS pattern which did not change from that shown in part 2 of Figure 3b (over the time scale of the experiment, 40 min in the linear regime). This indicates that large amplitude oscillatory shear induced a change in alignment of the cubic structure that was retained upon cessation of shear, although the rheological properties in a quiescent state were not affected by this symmetry change. A similar observation was previously made by us for sheared gels of the  $E_{40}B_{10}$  diblock in aqueous 0.2 M  $K_2SO_4$ , forming an fcc phase.<sup>21</sup> The recovery of the dynamic shear moduli was ascribed to



**Figure 4.** (a) dynamic shear moduli [ $(\circ)$   $G'$ ;  $(\blacksquare)$   $G''$ ] from simultaneous SAXS/rheology experiments for the gel subjected to different strain amplitudes (indicated) at a frequency  $\omega = 100 \text{ rad s}^{-1}$ . (b) SAXS patterns obtained concurrently, corresponding to the rheology as indicated by regime 1 or 2.

the local motion of defects, whereas SAXS probes the global alignment of the sample, which is "locked into" a new state by nonlinear flows.

The rheological response to strain steps at  $\omega = 100 \text{ rad s}^{-1}$  was similar to those at  $\omega = 10 \text{ rad s}^{-1}$ , as evident in Figure 4. Again, a transition in the symmetry of the SAXS pattern was observed at  $930 \pm 30 \text{ s}$ , corresponding to the onset of strain at  $\lambda = 100\%$ . In this case, the transition was from the state of partial alignment to complete alignment; i.e., the residual peaks at azimuthal angles  $\phi = 45^\circ$  with respect to the equator were eliminated by shear under these conditions, as shown in Figure 4b.

The changes in alignment of the gel following shear are summarized in Figure 5, which shows scans of the azimuthal SAXS intensity for the first-order reflections, achieved by integrating over narrow rings centered on the observed peaks, located at  $q^* = 0.062 \text{ \AA}^{-1}$ . The

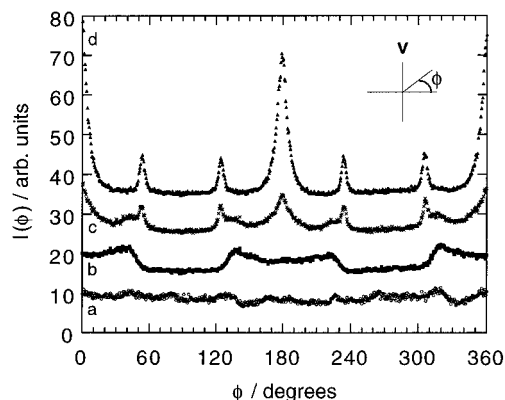


**Figure 5.** Scans of the SAXS intensity as a function of azimuthal angle indicating the changes in symmetry that occur during the shear protocol indicated in Figure 3 and 4. All patterns were acquired in the absence of large amplitude shear (at  $\lambda = 0.3\%$ ). Key: (a) sample as mounted; (b) sample following shear at  $\omega = 1 \text{ rad s}^{-1}$  ( $\lambda = 100\%$ ); (c) sample following shear at  $\omega = 10 \text{ rad s}^{-1}$  ( $\lambda = 100\%$ ); (d) sample following shear at  $\omega = 100 \text{ rad s}^{-1}$  ( $\lambda = 100\%$ ). The three upper curves have been shifted upward successively by 10 units.

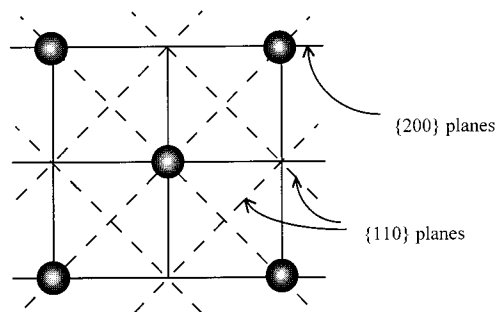


**Figure 6.** Projection along an  $\langle 001 \rangle$  direction of a bcc unit cell. Orientation of the  $\{200\}$  planes normal to the shear direction was observed at low frequencies.

initial unoriented state of the sample is confirmed by profile (a), which is essentially featureless. Following shear at  $\omega = 1 \text{ rad s}^{-1}$  ( $\lambda = 100\%$ ), broad peaks developed at  $\pm 45^\circ$  with respect to the equator (profile b). At a higher frequency, profile c in Figure 5 indicates that large amplitude oscillatory shear led to peaks at  $\pm 55^\circ$  with respect to the equator, with residual peaks from the initial orientation at  $45^\circ$  retained. These were removed after shear at  $\omega = 100 \text{ rad s}^{-1}$ ,  $\lambda = 100\%$  (d), which leads to strong broad peaks at 0 and  $180^\circ$  with four sharper peaks at  $\pm 55^\circ$ .

The SAXS pattern corresponding to the state following shear at  $\omega = 1 \text{ rad s}^{-1}$  (1 in Figures 3b and 4b) can be indexed on the basis of coexisting grains containing oriented  $\{110\}$  and  $\{200\}$  planes, as shown in Figure 6. Grains containing  $\{110\}$  planes are aligned parallel to the  $(\mathbf{v}, \mathbf{e})$  plane and those containing  $\{200\}$  planes are oriented in the  $(\nabla, \mathbf{e})$  plane, normal to the shear direction. This intriguing observation of planes in a "forbidden" orientation (i.e., normal to the shear direction) in a partially aligned sample has analogies with the results of Kornfield and co-workers on the lamellar phase in diblock copolymer melts. A forbidden "transverse" orientation (i.e. lamellae normal to the shear direction) was observed for samples oriented by planar oscillatory shear on the pathway to a final parallel alignment (lamellae in the  $(\mathbf{v}, \mathbf{e})$  plane).<sup>28</sup> In the cubic phase examined here, the "forbidden" orientation appears to be a stable (or long-lived metastable) state, rather than a transient because we observed it over the course of

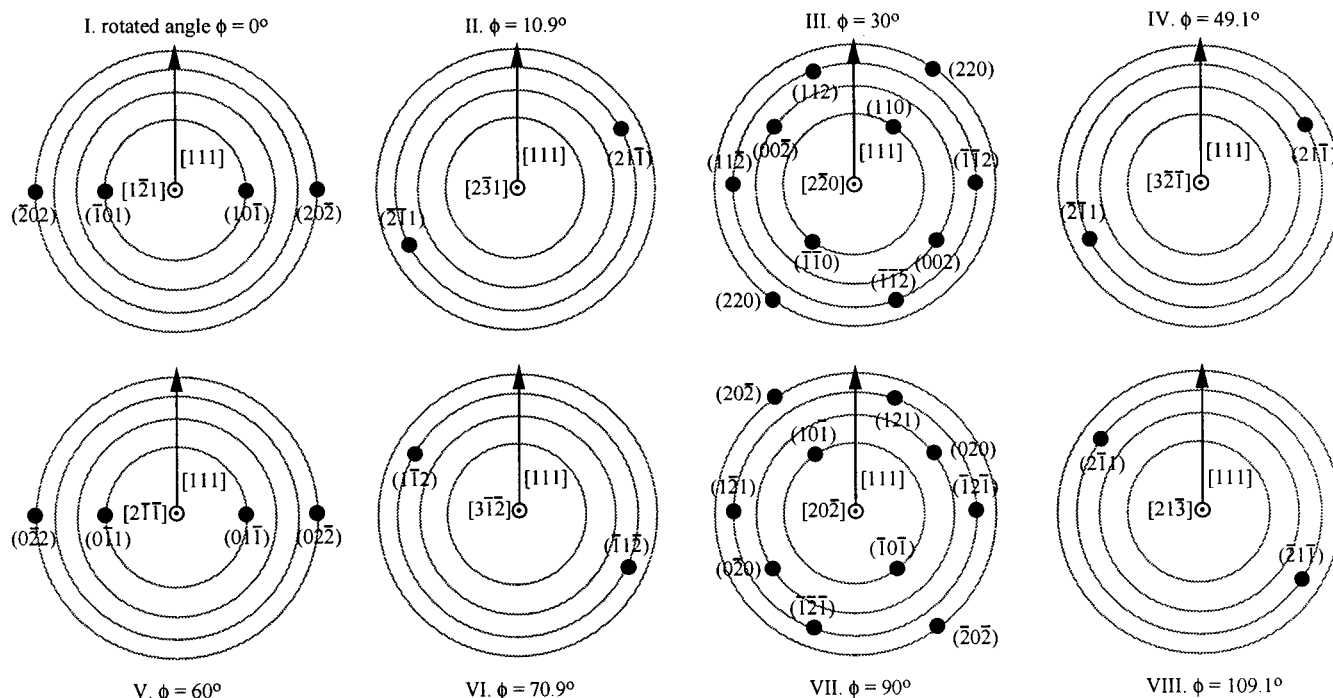


**Figure 7.** Indexation of the SAXS patterns obtained following large amplitude shearing at high frequencies. Patterns were obtained by rotating around the [111] direction by the angle  $\phi$  indicated.

45 min, and even when the orientation was subjected to shear up to  $\lambda = 10\%$  the alignment was retained.

On increasing strain amplitude to 100% at  $\omega = 10 \text{ rad s}^{-1}$  a transition occurred to a structure with the SAXS pattern given in part 2 of Figure 3b. This structure is perfected at  $\lambda = 100\%$ ,  $\omega = 100 \text{ rad s}^{-1}$ , as illustrated in Figure 4. The key to indexation of this pattern is the characteristic distribution of the ten  $\{211\}$  reflections, which are apparent in pattern 2 in Figure 4b. This pattern of  $\{211\}$  reflections is identical to that commonly observed for the "gyroid" (space group  $Ia\bar{3}d$ ) structure in block copolymers oriented by shear. It can be indexed on the basis that the [111] direction is coincident with the shear direction, and rotation by an angle  $\phi$  around the [111] direction leads to planes containing the [111] direction becoming coincident with the shear plane.<sup>29–31</sup> Unlike the gyroid structure, the bcc structure observed here has  $\{110\}$  and  $\{200\}$  reflections, together with  $\{211\}$  and  $\{220\}$  reflections, and these are indexed in Figure 7. A full rotation through  $\phi$  from 0 to  $360^\circ$  leads to this sequence of patterns being run through three times. Although a full complement of  $\{211\}$  reflections are apparent in SAXS pattern 2 in Figure 4b, only the equatorial  $\{220\}$  reflections can be discerned.

These results differ from those obtained previously for the bcc micellar phase formed by Pluronic triblocks in aqueous solution,<sup>8</sup> and PS-PI diblocks in concentrated solution in decane (a selective solvent for PI),<sup>23</sup> both systems being studied using SANS on samples sheared in a Couette cell. McConnell et al.<sup>23</sup> interpreted their data in accord with Ackerson and Clark,<sup>32</sup> who analyzed light scattering data for sheared polystyrene latex suspensions. This approach was later extended by Almdal et al.<sup>20</sup> to describe a twinned bcc phase in a diblock copolymer melt oriented by reciprocating shear. In this case, a  $\langle 111 \rangle$  direction lies along the shear direction, as in our model, but (110) planes are always stacked along the shear gradient direction. This differs

from our model in which these planes are rotated around the shear direction, producing the diffraction patterns in Figure 7 where (110) planes are brought into the diffracting condition only for particular rotation angles around the [111] direction. In the model for a twinned bcc structure,<sup>20</sup> developed for quantitative analysis by McConnell et al.,<sup>23</sup> the bcc crystal is twinned with the twinning plane perpendicular to the (110) planes, and the twins are oriented at  $35.3^\circ$  with respect to the shear direction. Our data indicates a distinct orientation mechanism, in which the structure is not twinned but rather corresponds to a "directionally oriented crystal", i.e., a crystal in which only one direction (the [111] direction) is selected by the shear field. The key feature is the distribution of  $\{211\}$  and  $\{220\}$  reflections, which differs from that evident in the data presented in earlier work.<sup>19,23,32</sup>

Patterns showing (110) reflections in the same arrangement as pattern 2 of Figure 4b were obtained previously by Koppi and co-workers<sup>20</sup> for block copolymer melts in an initially unoriented bcc phase. In common with these authors we associate this pattern with slip of a bcc structure in the three principal slip systems,  $\{110\}\langle 111 \rangle$ ,  $\{211\}\langle 111 \rangle$ , and  $\{321\}\langle 111 \rangle$ , as indicated in Figure 7. These also correspond to the principal slip systems for bcc metals,<sup>33</sup> indicating interesting commonality in the flow behavior of these "hard" and "soft" condensed matter systems. Considering the  $\{110\}$  reflections, the equatorial reflections arise from the  $\{211\}\langle 111 \rangle$  slip system ( $\phi = 0, 60^\circ$  in Figure 7), whereas the other four arise from the  $\{110\}\langle 111 \rangle$  system ( $\phi = 30, 90^\circ$  in Figure 7). Because the equatorial reflections are approximately four times more intense than the others, slip in  $\{211\}$  planes along a  $\langle 111 \rangle$  direction appears to be the predominant deformation mechanism in the  $E_{86}B_{10}$  gel. This system is also particularly active in bcc metals.<sup>33</sup> The fact that this orientation of our gel is obtained from a specimen in a state with a distinct prior orientation indicates that

deformation occurs through slip rather than via an affine deformation, at least for the relatively low shear rates accessed in our experiments. For bcc block copolymer melts, a shear-induced loss of translational order takes place at shear rates close to the inverse relaxation time of defects in the bcc phase, and affine elastic deformation, at much higher shear rates.<sup>20</sup> Patterns similar to those obtained by Koppi et al.<sup>20</sup> in these high frequency shear regimes have not been observed here, presumably due to the limited shear rates accessible with the rheometer employed. However, in separate experiments using a Couette cell to apply steady shear, in conjunction with SANS, evidence for (partial) shear-induced melting has been obtained at high shear rates.<sup>34</sup>

## Conclusions

The effect of shear on the alignment of the bcc phase in a gel of a diblock copolymer has been examined using simultaneous SAXS and rheology. The onset of strain at  $\lambda = 10\%$ , even though in the nonlinear regime, is insufficient to change the global alignment of the sample. However, shear at  $\lambda = 100\%$  causes transitions in the macroscopic orientation of the bcc gel. Locally, this corresponds to the displacement of the structure by one lattice unit and it appears that this condition has to be reached before macroscopic realignment occurs via slip, i.e., nonaffine deformation. Low-frequency shear (below  $\omega = 10 \text{ rad s}^{-1}$ ) leads to predominant alignment of  $\{200\}$  planes with normals parallel to the shear direction. At higher shear rates, a transition occurs to a different macroscopic orientation, in which the  $[111]$  direction is coincident with the shear direction. The diffraction pattern in this regime can be indexed by allowing for rotation of the reciprocal space about the  $[111]$  direction, which brings all observed  $\{110\}$ ,  $\{200\}$ ,  $\{211\}$ , and  $\{220\}$  reflections into the diffracting condition. The high degree of global alignment is apparent in SAXS patterns with multiple sharp reflections. Finally, it is evident that SAXS combined with simultaneous rheology provides an outstanding method for investigating the flow behavior of soft solids such as block copolymer gels.

**Acknowledgment.** We are grateful to the EPSRC (U.K.) for a grant (GR/K56117) that supported this work. Y.-Y.W. thanks the Government of the Republic of China for a research scholarship. We thank Dr. B. U. Komarschek for help in configuring the SAXS experiments at Daresbury.

## References and Notes

- Hamley, I. W. *The Physics of Block Copolymers*; Oxford University Press: Oxford, England, in press.
- Bates, F. S.; Fredrickson, G. H. *Annu. Rev. Phys. Chem.* **1990**, *41*, 525.
- Watanabe, H.; Yao, M.-L.; Sato, T.; Osaki, K. *Macromolecules* **1997**, *30*, 5905.
- Helfand, E.; Wasserman, Z. R. In *Developments in Block Copolymers*; Goodman, I., Ed.; Applied Science: London, 1982; Vol. 1.
- Almgren, M.; Brown, W.; Hvidt, S. *Colloid Polym. Sci.* **1995**, *273*, 2.
- Wanka, G.; Hoffmann, H.; Ulbricht, W. *Macromolecules* **1994**, *27*, 4145.
- Mortensen, K. *Europhys. Lett.* **1992**, *19*, 599.
- Mortensen, K.; Brown, W.; Nordén, B. *Phys. Rev. Lett.* **1992**, *68*, 2340.
- Mortensen, K.; Pedersen, J. S. *Macromolecules* **1993**, *26*, 805.
- Chu, B.; Zhou, Z. In *Polyoxyalkylene Block Copolymers*; Nace, V. M., Ed.; Nonionic Surfactants 60; Marcel Dekker: New York, 1996.
- Alexandridis, P.; Hatton, T. A. *Colloids Surf. A* **1995**, *96*, 1.
- Li, H.; Yu, G.-E.; Price, C.; Booth, C.; Hecht, E.; Hoffmann, H. *Macromolecules* **1997**, *30*, 1347.
- Yang, Z.; Pickard, S.; Deng, N.-J.; Barlow, R. J.; Attwood, D.; Booth, C. *Macromolecules* **1994**, *27*, 2371.
- Luo, Y. Z.; Nicholas, C. V.; Attwood, D.; Collett, J. H.; Price, D.; Booth, C. *Colloid Polym. Sci.* **1992**, *270*, 1094.
- Yang, Y.-W.; Ali-Adib, Z.; McKeown, N. B.; Ryan, A. J.; Attwood, D.; Booth, C. *Langmuir* **1997**, *13*, 1860.
- Tanodekaew, S.; Godward, J.; Heatley, F.; Booth, C. *Macromol. Chem. Phys.* **1997**.
- Ameri, M.; Attwood, D.; Collett, J. H.; Booth, C., *J. Chem. Soc., Faraday Trans.* **1997**, *93*, 2545.
- Alexandridis, P.; Olsson, U.; Lindman, B. *Langmuir* **1997**, *13*, 23.
- Almdal, K.; Koppi, K. A.; Bates, F. S. *Macromolecules* **1993**, *26*, 4058.
- Koppi, K. A.; Tirrell, M.; Bates, F. S.; Almdal, K.; Mortensen, K. *J. Rheol.* **1994**, *38*, 999.
- Pople, J. A.; Hamley, I. W.; Fairclough, J. P. A.; Ryan, A. J.; Yu, G.-E.; Booth, C. *Macromolecules* **1997**, *30*, 5721.
- Deng, N.-J.; Luo, Y. Z.; Tanodekaew, S.; Bingham, N.; Attwood, D.; Booth, C. *J. Polym. Sci. B* **1995**, *33*, 1085.
- McConnell, G. A.; Lin, M. Y.; Gast, A. P. *Macromolecules* **1995**, *28*, 6754.
- Yang, Y.-W.; Deng, N.-J.; Yu, G.-E.; Zhou, Z.-K.; Attwood, D.; Booth, C. *Langmuir* **1995**, *11*, 4703.
- Bras, W.; Derbyshire, G. E.; Ryan, A. J.; Mant, G. R.; Felton, A.; Lewis, R. A.; Hall, C. J.; Greaves, G. N. *Nucl. Instrum. Methods Phys. Res.* **1993**, *A326*, 587.
- The dynamic shear moduli  $G'$  and  $G''$  correspond to the real and imaginary components of the modulus, defined for an applied oscillatory strain in linear response. They are not defined if the viscoelastic response is nonlinear, i.e., if the oscillatory stress contains harmonics not present in the sinusoidal strain. In this case, it is more appropriate to plot the stress against strain in a Lissajous figure, as described elsewhere.<sup>27</sup> However, they do provide an indication of the shear thinning of the sample and are used in this context.
- Ohta, T.; Enomoto, Y.; Harden, J. L.; Doi, M. *Macromolecules* **1993**, *26*, 4928.
- Chen, Z.-R.; Kornfield, J. A.; Smith, S. D.; Grothaus, J. T.; Satkowski, M. M. *Science* **1997**, *277*, 1248.
- Schulz, M. F.; Bates, F. S.; Almdal, K.; Mortensen, K. *Phys. Rev. Lett.* **1994**, *73*, 86.
- Zhao, J.; Majumdar, B.; Schulz, M. F.; Bates, F. S.; Almdal, K.; Mortensen, K.; Hajduk, D. A.; Gruner, S. M. *Macromolecules* **1996**, *29*, 1204.
- Vigild, M. E.; Almdal, K.; Mortensen, K.; Hamley, I. W.; Fairclough, J. P. A.; Ryan, A. J. *Macromolecules*, submitted for publication.
- Ackerson, B. J.; Clark, N. A. *Phys. Rev. A* **1984**, *30*, 906.
- Hull, D.; Bacon, D. J. *Introduction to Dislocations*; Pergamon Press: Oxford, England 1984.
- Hamley, I. W.; Pople, J. A.; Booth, C.; Yang, Y.-W.; King, S. M. *Langmuir*, in press.

MA971561M